Ninth Canadian Conference on
Earthquake Engineering
Ottawa, Ontario, Canada
26-29 June 2007

SEISMIC EXCITED VIBRATION CONTROL OF CABLE-STAYED BRIDGE DURING CONSTRUCTION BY USING TMD AND ATMD

Y.K. Wen[1,2], T. Enomoto[1], L.M. Sun[2] and T. Yamamoto[1]

ABSTRACT

A cable-stayed bridge under construction has low structural damping and the system is not as stable as the completed one. The structure is easy to vibrate due to external excitation such as strong wind or earthquake. And even small earthquake can cause large force at bridge towers. It is necessary to adopt control countermeasures to reduce the seismic response for the safety of structure, especially when the bridge girders are at cantilever state. TMD (tuned mass damper) and ATMD (active tuned mass damper) have been proven to be effective schemes to control vibration of structure. As a complicated structure, a larger cable-stayed bridge under construction needs more than one mass damper to improve the control performance, and these dampers should be allocated at proper positions to have better performance. In the present study, a method based on H_2 control synthesis algorithm is used to design the multi-distributed TMDs and ATMDs. The 3rd Nanjing Bridge over Yangtze River (a large span cable-stayed bridge) under construction in China is used as an example. Three schemes of multi-distributed TMDs or ATMDs have been designed and simulated for the control of vertically, longitudinally and transversally excited vibration, and the performance is discussed. The simulation results show that the control schemes of multi-distributed TMDs and ATMDs optimized by H_2 control synthesis algorithm, which are properly designed, are effective for the seismic excited vibration control of large-cabled bridge under construction.

Introduction

A cable-stayed bridge under construction is easy to vibrate due to wind or earthquake. Except for having low structural damping the system is not as stable as the completed one. The superstructure of cable-stayed bridge under construction is supported by tower. Bridge deck extends outward in both directions from the tower, and there are no lateral or vertical constraints at the deck ends that would be present at the completed structure. Large forces at the tower may be caused when earthquake happens, which may even lead to collapse. It is necessary to adopt control countermeasures. Mass dampers, such as TMD and ATMD, have been proven to be effective schemes to control vibration of structure (Brownjohn, 2004, 2005). Furthermore, the equipment characteristics make mass dampers much fit for the vibration control of cable-stayed bridge under construction (Fujino, 1996, 2002; Soong, 2002).

As a spatial structure, a larger cable-stayed bridge will show complicated and different dynamical behavior depending on the excitation directions of earthquake. The mass damper should be properly designed for the seismic vibration control, and more than one mass damper is needed to improve the control performance, and these dampers should be allocated at proper positions. In this paper, the method based

[1] Dept. of Architecture and Building Engineering, Kanagawa University , Yokohama, Japan 221-8686
[2] State Key Laboratory for Disaster Reduction in Civil Engineering, Tongji University, Shanghai, China 200092

on H_2 control synthesis algorithm (Wen, 2006) is used to design the mass dampers (TMDs and ATMDs) distributed on cable-stayed bridge under construction. Three schemes of multi-distributed TMDs or ATMDs are designed and simulated for the control of vertically, longitudinally and transversally excited vibration by using the 3rd Nanjing Bridge over Yangtze River under construction as an example.

Formulations of Equations of Motion

For a finite element model (FEM) of a cable-stayed bridge, as an example the 3rd Nanjing Bridge under construction (Fig. 1), the seismically motion equation of structure can be repressed as

$$\mathbf{M}\ddot{\mathbf{X}}(s,t)+\mathbf{C}\dot{\mathbf{X}}(s,t)+\mathbf{K}\mathbf{X}(s,t)=-\mathbf{M}\Gamma\ddot{x}_g(t) \tag{1}$$

in which $\ddot{\mathbf{X}}$, $\dot{\mathbf{X}}$ and $\mathbf{X}$ = acceleration, velocity and displacement response vector with s being the position parameter of DOF; $\mathbf{M}$, $\mathbf{C}$ and $\mathbf{K}$ = mass, damping and stiffness matrix of the structure; Γ = a vector defining the loading of ground acceleration to the structure.

For a *n* degree of freedoms (DOF) model, structural displacement of vibation in Eq.1 can be expressed by generalized coordination as

$$\mathbf{X}(s,t)=\boldsymbol{\phi}\mathbf{Y}(t) \tag{2}$$

in which $\boldsymbol{\phi}$ = ($n\times n$) structural modes matrix; $\mathbf{Y}(t)$ =*n* general coordination vector. If $m=m_{TD}+m_{AD}$ mass dampers installed on the cable-stayed bridge, as shown in Fig. 2 (the installation direction can be freely defined). The motion equation of structure with mass dampers attached may be written as

$$\widehat{\mathbf{M}}\ddot{\mathbf{Y}}(t)+\widehat{\mathbf{C}}\dot{\mathbf{Y}}(t)+\widehat{\mathbf{K}}\mathbf{Y}(t)=-\boldsymbol{\phi}^T\mathbf{M}\Gamma\ddot{x}_g(t)+\boldsymbol{\phi}^T\Lambda^T\mathbf{f}_d(t) \tag{3}$$

in which $\mathbf{f}_d(t)=[f_{d1}(t)\quad f_{d2}(t)\quad\cdots\quad f_{dm}(t)]$ = m vector with $f_{di}(t)$ being the force from the *i*th mass damper; Λ = position and geological transfer matrix of mass dampers. $\widehat{\mathbf{M}}$, $\widehat{\mathbf{C}}$ and $\widehat{\mathbf{K}}$ = ($n\times n$) generalized mass, damping and stiffness matrices, respectively.

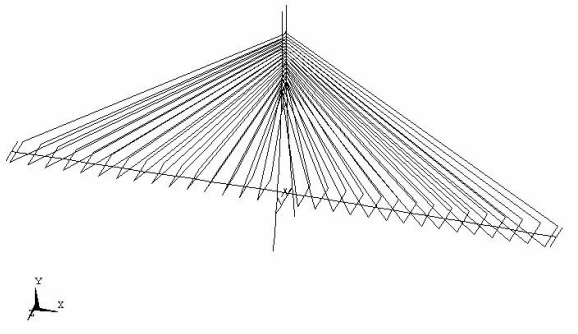

Figure 1. Finite element model of the 3rd Nanjing Bridge.

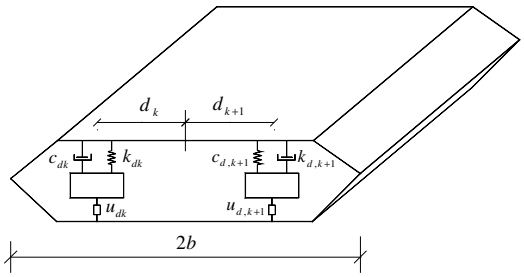

Figure 2. Schematic of bridge deck and mass damper.

The motion equation of mass dampers is

$$\mathbf{m}_d\ddot{\mathbf{x}}_d(t)+\mathbf{f}_d(t)=0 \tag{4}$$

where $\mathbf{m}_d=diag\left[m_{d1}\quad\cdots\quad m_{di}\quad\cdots\quad m_{dm}\right]$ = ($m\times m$) matrix with m_{di} being the mass of i th mass damper; $\ddot{\mathbf{x}}_d(t)=[\ddot{x}_{d1}(t)\quad\ddot{x}_{d2}(t)\quad\cdots\quad\ddot{x}_{dm}(t)]$ = m vector with $\ddot{x}_{di}(t)$ being the acceleration of i th mass damper. The force $f_{di}(t)$ to i th mass damper can be represented as

$$f_{di}(t)=c_{di}(\dot{x}_{di}-\dot{x}_i)+k_{di}(x_{di}-x_i)+\varepsilon m_{di}g\,\mathrm{sgn}[\dot{x}_{di}]-u_{di}(t) \tag{5}$$

where x_i = displacement of main structure at the position of the i th mass damper installed, which can be represented as $x_i = \Lambda \mathbf{X}(s,t)$; ε =coefficient of friction; c_{di} , k_{di} , $u_{di}(t)$ = damping , stiffness and actuation force of i th mass damper.

Submitting Eq.5 into Eq.3 and Eq.4 and rewriting Eq.3 and Eq.4 with compact form, the equation of motion of system is

$$\widehat{\mathbf{M}}^s\ddot{\widehat{\mathbf{Z}}} + \widehat{\mathbf{C}}^s\dot{\widehat{\mathbf{Z}}} + \widehat{\mathbf{K}}^s\widehat{\mathbf{Z}} + \widehat{\mathbf{H}}\mathbf{c}_d\widehat{\mathbf{H}}^T\dot{\widehat{\mathbf{Z}}} + \widehat{\mathbf{H}}\mathbf{k}_d\widehat{\mathbf{H}}^T\widehat{\mathbf{Z}} = \widehat{\mathbf{\Phi}}\ddot{x}_g(t) + \widehat{\mathbf{H}}\mathbf{u} \tag{6}$$

in which

$$\widehat{\mathbf{Z}} = [\mathbf{Y}' \quad \mathbf{x}_d']'; \widehat{\mathbf{M}}^s = \begin{bmatrix} \widehat{\mathbf{M}} & 0 \\ 0 & \mathbf{m}_d \end{bmatrix}; \widehat{\mathbf{C}}^s = \begin{bmatrix} \widehat{\mathbf{C}} & 0 \\ 0 & 0 \end{bmatrix}; \widehat{\mathbf{K}}^s = \begin{bmatrix} \widehat{\mathbf{K}} & 0 \\ 0 & 0 \end{bmatrix} \tag{7}$$

$$\widehat{\mathbf{H}} = \begin{bmatrix} -\boldsymbol{\phi}^T\mathbf{D}^T\mathbf{T}^T \\ I \end{bmatrix}; \widehat{\mathbf{\Phi}} = \begin{bmatrix} -\boldsymbol{\phi}^T\mathbf{M}\Gamma \\ 0 \end{bmatrix} \tag{8}$$

In the state space, Eq.6 becomes

$$\dot{\mathbf{x}} = \mathbf{A}\mathbf{x} + \mathbf{B}\mathbf{u} + \mathbf{E}\mathbf{w} \tag{9}$$

where $\mathbf{x}$ = 2p state vector with $p = n + m$; $\mathbf{A}$ = (2p×2p) system matrix; $\mathbf{B}$ = (2p×m) control location matrix; and $\mathbf{E}$ = (2p×s) excitation influence matrix, given respectively, by

$$\mathbf{x} = \begin{Bmatrix} \mathbf{Z} \\ \dot{\mathbf{Z}} \end{Bmatrix}; \mathbf{A} = \begin{bmatrix} \mathbf{0}_p & \mathbf{I}_p \\ -\mathbf{M}^{-1}\mathbf{K}^* & -\mathbf{M}^{-1}\mathbf{C}^* \end{bmatrix}; \mathbf{B} = \begin{bmatrix} \mathbf{0}_{p\times m} \\ \mathbf{M}^{-1}\mathbf{H} \end{bmatrix}; \mathbf{E} = \begin{bmatrix} \mathbf{0}_p \\ \mathbf{M}^{-1} \end{bmatrix} \tag{10}$$

in which $\mathbf{K}^* = \mathbf{K}^s + \mathbf{H}\mathbf{k}_d\mathbf{H}^T$, $\mathbf{C}^* = \mathbf{C}^s + \mathbf{H}\mathbf{c}_d\mathbf{H}^T$. In general, the l -dimensional controlled output vector $\mathbf{z}$ and q -dimensional measured output vector can be expressed, respectively, by

$$\mathbf{z} = \mathbf{C}^z\mathbf{x} + \mathbf{D}^z\mathbf{u} + \mathbf{E}^z\mathbf{w} \tag{11}$$

$$\mathbf{y} = \mathbf{C}^y\mathbf{x} + \mathbf{D}^y\mathbf{u} + \mathbf{E}^y\mathbf{w} \tag{12}$$

in which $\mathbf{C}^z, \mathbf{D}^z, \mathbf{E}^z, \mathbf{C}^y, \mathbf{D}^y$ and $\mathbf{E}^y$ are matrices with appropriate dimensions. If only the state variables (displacement and velocity) are measured, then $\mathbf{D}^y$ = $\mathbf{E}^y$ = 0. Eq.12 is the general expression also including acceleration measurement and the same remark applies to the controlled output in Eq.11.

Design Method Based on H_2 Control Synthesis Algorithm

Parameters Design of multi-distributed TMDs

The frequency and damping ratio of one TMD can be optimized by traditional design method in which dynamical magnification coefficient is used to define the performance index and the main structure is modeled as an SDOF structure (Warburton,1982). For a spatial structure, more than one TMD is used, and the TMDs are distributed in different positions to improve the performance. In such case, the traditional method can not be used because of its limitation. In the paper, H_2 performance is adopted to optimize the parameters of multi-distributed TMDs, which is easy to select the physical constant, such as displacement, acceleration, internal force and stress, etc., and to build the energy of structural response as performance index.

If only TMDs are used for the vibration control of cable-stayed bridge and the frequencies and damping ratios are unknown, the state equation Eq.9 and Eq.11 can be rewritten as

$$\dot{\mathbf{x}} = \mathbf{A}(\boldsymbol{\delta})\mathbf{x} + \mathbf{E}\mathbf{w} \; ; \; \mathbf{z} = \mathbf{C}^z(\boldsymbol{\delta})\mathbf{x} + \mathbf{E}^z\mathbf{w} \tag{13}$$

in which $\boldsymbol{\delta} \in \Delta$ is the variables of parameters with Δ being the region for possible parameters. Then the H_2 performance of the controlled output vector $\mathbf{z}$ can be formed. If the excitation w is assumed to be a

white noise vector, the H_2 performance $\|T(\boldsymbol{\delta}, s)\|_2$ with $\mathbf{T}(\boldsymbol{\delta}, s)$ being the transfer matrix from w to the control output z and s being the Laplace parameter, is defined as the root-mean square (RMS) of the controlled output z, i.e.

$$\|T(\boldsymbol{\delta}, s)\|_2^2 = \lim_{T\to\infty}\frac{1}{T}\int_0^T E\left[\mathbf{z}^T\mathbf{z}\right]dt = \frac{1}{2\pi}\int_{-\infty}^{+\infty} tr\left[T^H(\boldsymbol{\delta}, j\omega)T(\boldsymbol{\delta}, j\omega)\right]d\omega \tag{14}$$

in which a super *H* denotes the complex conjugate; *E*[] and *tr*[] indicate the expected value and the trace of the matrix in the racket respectively.

The optimization of the unknown parameters of multi-distributed TMDs based on H_2 performance is to find the optimal value of variables $\boldsymbol{\delta}$ when the H_2 performance gets its minimum value. It is assumed that the search of the optimal parameters is a convex problem. Then linear matrix inequality (LMI) can be used for the H_2 performance constraints and it is very convenient to obtain the resolution by using the LMI Toolbox of MATLAB (Yang, 2002).

Control Strategies of multi-distributed ATMDs

An ATMD should be tuned to one of the structural modal frequency and its damping ratio should also be the optimal value. Usually, the frequency and damping ratio of the TMD are adopted by ATMD, further the control gain of ATMD is designed. In the paper, based on the results of TMDs optimized by H_2 performance, LQG method is used for the design of control gain. The LQG method in time domain is equivalent to H_2 theory in frequency domain.

Because a cable-stayed bridge has a high number of DOF, a reduced order design mode must be built before the active control gain is designed. With assumption of the installation of mass dampers without changing the modal shape remarkably, modal supposition method is efficient to reduce the system mode by selecting the r modal shapes that contribute the structural response mainly (Schemmann, 1997). The state equation of the reduced mode can be written as

$$\dot{\mathbf{x}}_r = \mathbf{A}_r\mathbf{x}_r + \mathbf{B}_r\mathbf{u} + \mathbf{E}_r\mathbf{w} \tag{15}$$

$$\mathbf{z} = \mathbf{C}_r^z\mathbf{x}_r + \mathbf{D}_r^z\mathbf{u} + \mathbf{E}_r^z\mathbf{w} \tag{16}$$

$$\mathbf{y} = \mathbf{C}_r^y\mathbf{x}_r + \mathbf{D}_r^y\mathbf{u} + \mathbf{E}_r^y\mathbf{w} + \mathbf{v} \tag{17}$$

in which $\mathbf{x}_r = 2a$ state vector with $a = r + m$; $v = q$ vector of measurement noise. The dimension and meanings of the other vectors or matrices in Eq.15~Eq.17 are similar to and can refer to that of Eq.9 ~ Eq.12.

Based on the assumption that the excitation w and the measurement noise v are uncorrelated Gaussian white noise process, the control design procedure for LQG method is divided into two parts: the design of controller to obtain the feedback control gain $\mathbf{K}_u$ and the design of observer to obtain the estimated state $\hat{\mathbf{x}}_r$ (Wu, 1998). The optimal controller is obtained as $\mathbf{u} = -\mathbf{K}_u\mathbf{x}_r$. The feedback control gain is obtained by minimizing the quadratic objective function

$$J = \lim_{\tau\to\infty}\frac{1}{\tau}\mathrm{E}\left[\int_0^\tau\left\{\overline{\mathbf{z}}^T\mathbf{Q}\overline{\mathbf{z}} + \mathbf{u}^T\mathbf{R}\mathbf{u}\right\}dt\right] \tag{18}$$

in which $\overline{\mathbf{z}} = \mathbf{z} - \mathbf{E}_r^z\mathbf{w}$; $\mathbf{Q}$ and $\mathbf{R}$ = weighting matrices. The modulation of control force **u** and the controlled output ***z*** can be achieved by choosing proper $\mathbf{Q}$ and $\mathbf{R}$. Because of the limited number of sensors, an observer should be developed to estimate the state feedback, and Kalman-Bucy filter is used to estimate the state $\mathbf{x}_r$.

Control scheme and numerical Simulations

FEM and excitation model

The 3rd Nanjing Bridge over Yangtze River under construction is adopted as an example. The bridge is composed of two steel towers and the main span is 648m in length. A FEM of the 3rd Nanjing Bridge with two cantilevers state was built, in which beam elements, truss elements and rigid links were employed (Fig.1). The total number of DOF was 1188, and by applying constraints (condensing out the rigid links and supports constraints) the result model had 756 DOF for the superstructure. The non-linear static analysis was carried out and the system matrixes, including mass matrix and stiffness matrix, were abstracted based on the analysis results, which would be used for the control design.

The seismic excited response of the cable-stayed bridge was simulated. According to the earthquake resistance design criterion of the 3rd Nanjing Bridge under construction, artificial seismic waves of site ground accelerations were used for the simulation. The selected vertical and horizontal rock waves (Fig. 3) having maximum acceleration with a 10 percent probability of being exceeded in 100-year were assumed to be applied at the support respectively, and the effects of the soil-structure interaction were neglected.

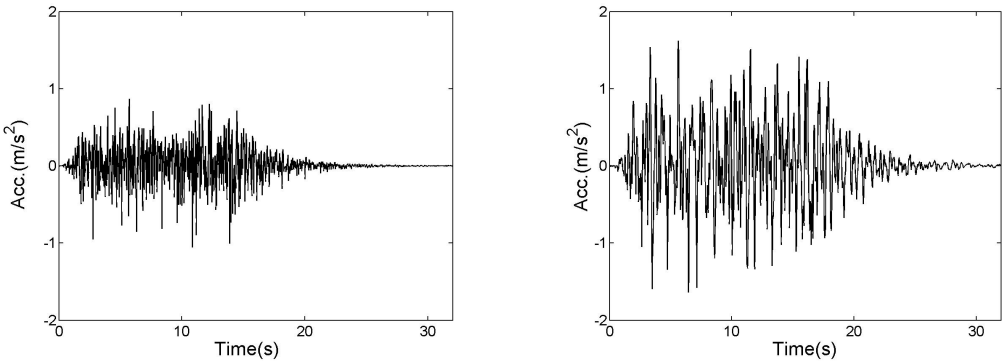

(a) Vertical wave (b) Horizontal wave

Figure 3. Artificial seismic waves for the 3rd Nanjing Bridge under construction.

Control scheme

Three different schemes were designed by using mass dampers (TMDs and ATMDs) for the vibration control of the cable-stayed bridge excited in vertical (vertical wave), longitudinal (horizontal wave) and transversal (horizontal wave) direction. Considering the practical application, two mass dampers were adopted and distributed at the end of the deck cantilevers for the control analysis. Their total mass was 20t which was about 1% of the effective mass of the structure that calculated with the first modal shape. The shear force and moment of two tower legs at the deck level $[F_1 \quad F_2 \quad M_1 \quad M_2]$ were selected to form the control output vector $\mathbf{z}$, with which the control objective was built for the design of mass dampers. To measure the relevant performance of the mass dampers, the indices were defined as follows:

$$J_1 = \max_t \left|x_c(t)\right| \Big/ x_{0c}^{\max} \; ; \; J_2 = \max_t \left|x_l(t)\right| \Big/ x_{0l}^{\max} \; ; \; J_3 = \max_{i,t} \left|F_i(t)\right| \Big/ F_0^{\max} \; ; \; J_4 = \max_{i,t} \left|M_i(t)\right| \Big/ M_0^{\max} \tag{19}$$

$$J_5 = \left\|x_c(t)\right\| \Big/ \left\|x_{0c}\right\| ; \; J_6 = \left\|x_l(t)\right\| \Big/ \left\|x_{0l}\right\| ; \; J_7 = \max_i \left\{ \left\|F_i(t)\right\| \Big/ \left\|F_0\right\| \right\} ; \; J_8 = \max_i \left\|M_i(t)\right\| \Big/ \left\|M_0\right\| \tag{20}$$

$$J_9 = \max_{i,t} \left|s_{d,i}(t)\right| \Big/ x_0^{\max} \; ; \; J_{10} = \sum_i \max_t \left|\dot{s}_{d,i}(t) f_i(t)\right| \tag{21}$$

$$J_{11}=\max_i \left\|s_{d,i}(t)\right\| \Big/ \left\|x_0^{\max}\right\|;\ J_{12}=\sum_i \left(\frac{1}{T}\int_0^T \dot{s}_{d,i}(t) f_i(t)dt\right)^{1/2} \tag{22}$$

where x: displacement at the deck ends of cantilever; subscript *c* and l indicate middle-span and side-span; subscript 0 indicates response without control; F_i and M_i: shear force and moment of lth tower leg; $s_{d,i}$, $\dot{s}_{d,i}$ and $f_i(t)$: actuator displacement, velocity and force of ith ATMD; $\|\square\|$: RMS value. The actuator capacity constraints of ATMDs were the maximum control force $\max_i \left|f_i(t)\right| \le 100$ kN and the maximum control stroke $\max_i \left|x_{d,i}(t)\right| \le 1.5$ m. The indices except for J_{10} and J_{12} were for the performance measurement of TMDs and all the indices would be used for the performance measurement of ATMDs.

Performance of multi-distributed TMDs and ATMDs

Vertically excited vibration control

When the cable-stayed bridge was excited in vertical direction, the vertical vibration of deck and coupled longitudinal vibration of tower would be induced. The dynamical response was mainly contributed by vertical modal shapes, and those in the former 20 structural modes are given in Table 1. To reduce the shear force and moment of tower at deck level, ATMDs were adopted and installed vertically for the multi-modal shapes vibration (Fig.3). The directions of displacement, shear force and moment in Eq.19 and Eq.20 were y, x and z respectively.

The contribution degree of the modes is different depending on the frequency spectra characteristics of seismic, and that of one position of the bridge can be calculated. However, an ATMD can only work in a narrow frequency band and are not in response to the modes with high frequencies. In the paper, it was considered the vertical modal shapes in the former 20 modes (Table 1) were enough for the vertically excited vibration control by ATMDs, and the modal shapes were used to form the design model of multi-distributed ATMDs too. 9 accelerometers were employed in the sample system, 7 of them were distributed on the deck to measure the vertical acceleration and the other two were located on each of the two tower legs to measure the longitudinal acceleration (Fig. 3).

Table 1 Modal shapes contributed to the vertically excited vibration

Mode	Frequency(Hz)	Modal shape description
1	0.2390	1st vert. deck+long. tower
4	0.5348	2nd vert. deck
5	0.7183	3rd vert. deck
8	1.0868	4th vert. deck+long. tower
9	1.1672	5th vert. deck
11	1.2817	6th vert. deck+long. tower
13	1.3695	7th vert. deck+long. tower
14	1.7885	8th vert. deck
17	2.1662	9th vert. deck
19	2.5020	10th vert. deck+long. tower

The frequencies of ATMDs were tuned to mode 1 and the frequency ratios and damping ratios of the multi-distributed ATMDs were optimized by using H_2 performance firstly. The optimal frequency

ratios of ATMDs were 0.964, 1.030 and the optimal damping ratios were 0.031, 0.030. For the feedback gain design, weighting matrix $\mathbf{R} = diag[1 \quad 1]$ of actuating volts (with a span of 10 volts) and $\mathbf{Q} = 60 \times \mathrm{I}_{4\times4}$ of output vector $\mathbf{z}$ which was normalized firstly were chosen, and for the observer design the seismic excitation and measurements were assumed to be identically distributed, statistically independent white noise with the power spectral density ratio of 25. The eigenvalue analysis was carried out during the controller design and system simulation. Both the controller and the closed-loop system composed of the controller and structural modal were assured to be stable.

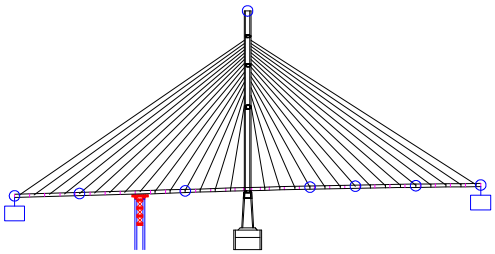

Figure 3. Distribution of mass dampers and sensors(O – sensor ; □– mass damper)

The performance of the designed multi-distributed ATMDs and the corresponding actuator requirements are presented in column 2 and column 6 of Table 2. Because ATMDs can control multi-mode vibration, the vertical peak response of deck is reduced by almost 20%~30%. As a result, the coupled longitudinal response of bridge tower can also be reduced. The peak value and norm value of shear force and moment of tower at deck level is reduced by 20%~30% (table 2). The time history responses of the shear force and moment of tower at deck level are showed in figure 4.

Table 2. Performance and requirements of multi-distributed TMDs and ATMDs.

Criteria	Peak response			Criteria	RMS response		
	Vert.	Long.	Trans.		Vert.	Long.	Trans.
J_1	0.797	0.287	0.895	J_5	0.8897	0.281	0.894
J_2	0.704	0.273	0.868	J_6	0.7999	0.275	0.865
J_3	0.759	0.826	0.668	J_7	0.7415	0.721	0.507
J_4	0.711	0.721	1.704	J_8	0.6745	0.744	1.289
J_9	3.685	5.297	3.85	J_{11}	3.620	6.745	4.161
J_{10},kN m/s	137.4			J_{12},kN m/s	15.96		
$\max_i \lvert x_{d,i}(t) \rvert$, m	0.44	1.07	1.11	$\max_i \lvert f_i(t) \rvert$, kN	95.03		

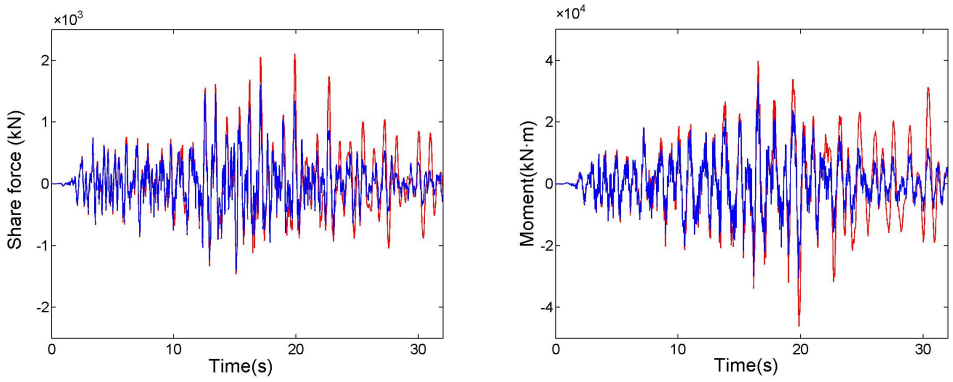

(a) shear force (b) moment

Figure 4. Simulated response of tower at deck level to vertical seismic with and without control of multi-distributed ATMDs.

Longitudinally excited vibration control

When the cable-stayed bridge was excited along the bridge, structural response was longitudinal vibration of deck and longitudinal vibration of tower and coupled vertical vibration of deck The modal shapes contributed to the vibration in the former 20 structural modes are given in Table 3. However, structural dynamical analysis under longitudinal seismic excitation showed shear force (x-direction) and moment (z-direction) were mainly contributed by the longitudinal modal shape of deck and tower (mode 19). To reduce the shear force and moment of tower at deck level, TMDs were installed longitudinally at the end of deck. The directions of displacement, shear force and moment in Eq.19 and Eq.20 are x, x and z respectively.

Table 3. Modal shapes contributed to the longitudinally excited vibration.

Mode	Frequency(Hz)	Modal shape description
1	0.2390	1st vert. deck+long. tower
8	1.0868	4th vert. deck+long. tower
11	1.2817	6th vert. deck+long. tower
13	1.3695	7th vert. deck+long. tower
19	2.5020	long. deck+long. tower

The multi-distributed TMDs were tuned to mode 19. The frequency ratios optimized by H_2 performance were 0.985Hz and 1.013Hz, and the optimal damping ratios were 0.012 and 0.012. The performance of multi-distributed TMDs is given in the column 3 and column 7 of Table 2. Fig 5 presents the time history response of shear force and moment of tower at deck lever with and without control. The results of performance indices show that the peak and norm value of shear force and moment tower at deck level are reduced by almost 20%~30%. For the longitudinal vibration of deck is mainly contributed by the mode 19, multi-distributed TMDs is more effective for the control of deck longitudinal displacement which is reduced by more than 70% (table 2).

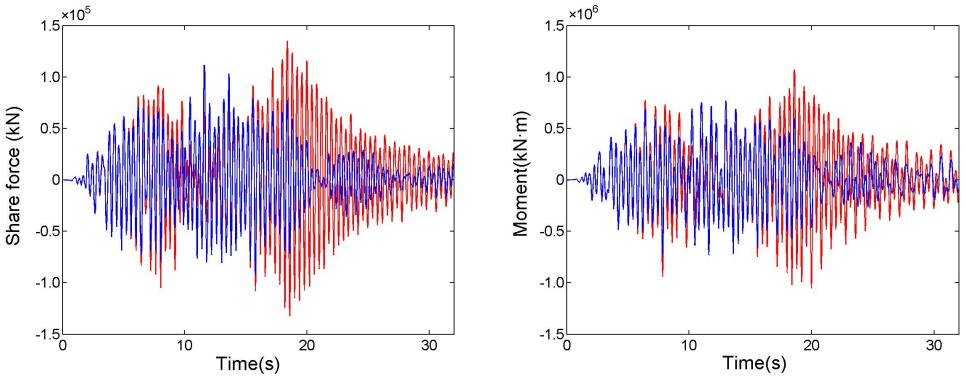

(a) shear force (b) moment

Figure 5. Simulated response of tower at deck level to longitudinal seismic with and without control of multi-distributed TMDs.

Transversally excited vibration control

When the cable-stayed bridge was excited in transversal direction, structural response would be transversal vibration of deck and transversal vibration of tower and coupled torsional vibration of deck. Table 4 presents the modal shape contributed to the structural vibration in former 20 structural modes. Structural dynamical analysis under transversal seismic excitation showed the shear force (z-direction) was mainly contributed by the transversal modal shape of deck and tower (mode 20) and had a large value, and the moment (x-direction) that was mainly contributed by lower modal shapes had a rather smaller value comparing with the shear force. To reduce the shear force of tower at deck level, TMDs were adopted and installed transversally on the deck. The directions of displacement, shear force and moment in Eq.19 and Eq.20 are z, z and x respectively.

Table 4. Modal shapes contributed to the transversally excited vibration.

Mode	**Frequency(Hz)**	**Modal shape description**
2	0.3846	1st trans. Deck
3	0.4556	2nd trans. Deck
6	0.9235	1st tors. deck+trans. tower
10	1.1721	3rd tors. deck+trans. tower
18	2.3763	3rd trans. Deck
20	2.5414	4th trans. Deck+tans. tower

The multi-distributed TMDs were tuned to mode 20. The frequency ratios optimized by H_2 performance were 0.977, 1.017, and the optimal damping ratios were 0.017, 0.019. Column 4 and column 8 in Table 2 present the performance of multi-distributed TMDs for the transversally excited vibration control. The time history response of shear force and moment of tower at level is showed in Fig. 6. It is showed that the multi-distributed TMDs is effective for the control of displacement of deck end and the control of shear force of tower at deck level. Peak value of the shear force is reduced by more than 30% and norm value is reduced by almost 50%. Because of the couple effect of modal shapes, the moment response of tower at deck level is a little enlarged. However, the moment value that induced by the transversal seismic excitation is rather small (Fig. 6), so the enlargement do not effect the control performance.

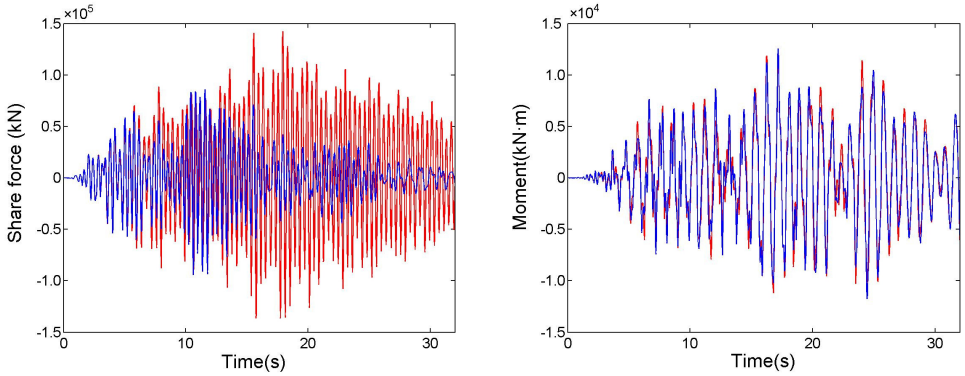

(a) shear force (b) moment

Figure 6. Simulated response of tower at deck level to transversal seismic with and without control of multi-distributed TMDs.

Conclusions

To investigate the seismic excited vibration control of a large cable-stayed bridge under construction, multi-distributed mass dampers are adopted as control devices. A structural model consisted of a cable-stayed bridge with distributed mass dampers was established first. For the limitation of traditional methods, the H_2 control synthesis algorithm was used to optimize the parameters of multi-distributed mass dampers. Three schemes of multi-distributed TMDs or ATMDs were designed and simulated for the vertical, longitudinal and transversal seismic excited vibration control respectively based on the linear model. Simulation results show that multi-distributed ATMDs should be used for the vertically excited vibration because of the multi-mode contribution of the structural response. As only one modal shape mainly contributes to the force response at key positions of the cable-stayed bridge under construction when excited in longitudinal and transversal direction, multi-distributed TMDs can also have good performance for the excited vibration.

Acknowledgments

This research is a part of the “Excellent Frontier Research Project on Risk Management System Combined with Hard and Soft Measures for Natural Disaster Risk Reduction” in Kanagawa University, through the grant in aid from “Ministry of education, culture, sports, science and technology”. The research is also partially supported by the fund of Chinese Ministry of Education (Grant No.GG-560-10247). The help by Professor Wang J.J of Tongji Univ. is greatly acknowledged.

References

Brownjohn, J.M.W., P. Fok, M. Roche, and P. Omenzetter. 2004, Long span steel pedestrian bridge at Singapore Changi Airport. Part 2: Crowd loading tests and vibration mitigation measures. *The Structural Engineer*, Vol. 82(16): 38-34.

Brownjohn, J. M. W. and N. F. Tao, 2005. Vibration excitation and control of a pedestrian walkway by individuals and crowds. *Journal of Shock and Vibration*, Vol. 12(5), 333-374.

Fujino Y., T.T.Soong and Jr B. F.Spencer, 1996. Structural control: basic concepts and applications. *The Proceedings of the 1996 ASCE Structures Congress,* Chicago, Illinois, April 15–18.

Fujino Y., 2002. Vibration control and monitoring of long–span bridge—recent research, developments and practice in Japan, *Journal of Constructional Steel Research*, 58. 71-97.

Schemmann A.G., 1997. Modeling and active control of cable-stayed bridges subject to multiple-support excitation, *PhD thesis,* Standford University.

Soong T.T. and Jr B.F.Spencer, 2002. Supplemental energy dissipation: state-of-the-art and state-of-the-practice, *Engineering Structures*24. 243-259.

Warburton G.B. and E.O.Ayorinde, 1982. Optimum absorber parameters for simple systems, *Earthquake Engineering and Structural Dynamics* 8, 197-217.

Wen Y.K. and L.M. Sun, 2006. Wind-induced vibration control of cable-stayed bridge during construction by using TMD and ATMD, *4th World Conference on Structural Control and Monitoring,* San Diego, July 11-13

Wu J.C. and J.N. Yang, 1998. Active control of transmission tower under stochastic wind, *Journal of Structural Engineering*124(11), 1302-1312.

Yang, J.N., S. Lin, J-H. Kim, and A.K. Agrawal, 2002. Optimal design of passive energy dissipation systems based on H_∞ and H_2 performances, *Earthquake Engineering and Structural Dynamics,* 31, 921-936.